You might find this additional information useful...

This article cites 49 articles, 12 of which you can access free at:
http://ajpregu.physiology.org/cgi/content/full/295/6/R2041#BIBL

Updated information and services including high-resolution figures, can be found at:
http://ajpregu.physiology.org/cgi/content/full/295/6/R2041

Additional material and information about *American Journal of Physiology - Regulatory, Integrative and Comparative Physiology* can be found at:
http://www.the-aps.org/publications/ajpregu

This information is current as of December 20, 2008 .

Rapid changes in glutamate levels in the posterior hypothalamus across sleep-wake states in freely behaving rats

Joshi John, Lalini Ramanathan, and Jerome M. Siegel

Neurobiology Research (151A3), Veterans Affairs Greater Los Angeles Health Care System, North Hills; and Department of Psychiatry and Brain Research Institute, University of California at Los Angeles, Los Angeles, California

John J, Ramanathan L, Siegel JM. Rapid changes in glutamate levels in the posterior hypothalamus across sleep-wake states in freely behaving rats. *Am J Physiol Regul Integr Comp Physiol* 295: R2041–R2049, 2008. First published September 24, 2008; doi:10.1152/ajpregu.90541.2008.— The histamine-containing posterior hypothalamic region (PH-TMN) plays a key role in sleep-wake regulation. We investigated rapid changes in glutamate release in the PH-TMN across the sleep-wake cycle with a glutamate biosensor that allows the measurement of glutamate levels at 1- to 4-s resolution. In the PH-TMN, glutamate levels increased in active waking (AW) and rapid eye movement (REM) sleep compared with quiet waking and nonrapid eye movement (NREM) sleep. There was a rapid (0.6 ± 1.8 s) and progressive increase in glutamate levels at REM sleep onset. A reduction in glutamate levels consistently preceded the offset of REM sleep by 8 ± 3 s. Short-duration sleep deprivation resulted in a progressive increase in glutamate levels in the PH-TMN, perifornical-lateral hypothalamus (PF-LH), and cortex. We found that in the PF-LH, glutamate levels took a longer time to return to basal values compared with the time it took for glutamate levels to increase to peak values during AW onset. This is in contrast to other regions we studied in which the return to baseline values after AW was quicker than their rise with waking onset. In summary, we demonstrated an increase in glutamate levels in the PH-TMN with REM/AW onset and a drop in glutamate levels before the offset of REM. High temporal resolution measurement of glutamate levels reveals dynamic changes in release linked to the initiation and termination of REM sleep.

rapid eye movement sleep; histamine; microdialysis; biosensor; cortex

VARIOUS STUDIES HAVE IMPLICATED glutamatergic mechanisms in the control of sleep-wake states. In vitro experiments reported a differential glutamate release in brain regions of long-sleep and short-sleep mice (11). Glutamate release was higher during wakefulness than during sleep in the pedunculopontine tegmental nucleus (22), whereas enhanced glutamate release during rapid eye movement (REM) sleep was observed in the rostromedial medulla (24). Paradoxical sleep deprivation increased the content of glutamate and glutamine in the rat cerebral cortex (3).

Glutamate excites both cortical and subcortical neurons and enhances the in vivo release of histamine (HA) through presynaptic *N*-methyl-D-aspartate receptors in the anterior hypothalamus of the rat (32). Single cell recording and microdialysis experiments demonstrate that HA cell activity is reduced in nonrapid eye movement (NREM) sleep and REM sleep compared with waking (7, 20). We hypothesized that changes in glutamate release in the posterior hypothalamus histaminergic tuberomammillary nucleus (PH-TMN) and in the terminal

regions of HA neurons could affect HA release and sleep-wake states. Dysfunction of the Hcrt system produces the sleep disorder narcolepsy (35, 38, 44). Hcrt neurons contain glutamate as a cotransmitter (1). Hcrt effects on sleep-wake state distribution are to some extent mediated by the HA system (17).

The short duration of sleep-wake transition and sleep-wake states makes it difficult to accurately measure the time course of transmitter release across each state using the standard microdialysis-HPLC technique, where samples are collected over a 3- to 5-min interval. In the present study, we used a newly developed glutamate sensor to measure changes in glutamate levels across sleep-wake states with a temporal resolution of 3–5 s (16). We monitored glutamate levels across the sleep-wake cycle in the PH-TMN and compared it with changes in the perifornical-lateral hypothalamus (PF-LH) and cortical areas in freely moving rats. A preliminary presentation of the data has been made (21).

MATERIALS AND METHODS

Male Sprague-Dawley rats weighing between 300 and 400 g were used for this study. All procedures were done in accordance with the National Research Council Guide for the Care and Use of Laboratory Animals. Animal protocols were approved by the Institutional Animal Care and Use Committee (IACUC) of the University of California at Los Angeles and by the IACUC of the Veterans Administration Greater Los Angeles Health Care System. The rats were kept on 12h:12-h light-dark cycle (6:00 A.M. lights on, 6:00 P.M. lights off), ambient temperature 24 ± 1°C, with food and water available ad libitum. Rats were anesthetized with ketamine-xylazine (80:10 mg/kg ip). Electrodes for the assessment of sleep-wake parameters were chronically implanted under aseptic conditions, as described previously (18). In brief, bilateral stainless steel screw electrodes were threaded through the skull over the frontal and parietal cortex to record electroencephalogram (EEG). One screw electrode threaded through the midline of the frontal bone was used as ground. Teflon-coated multistranded stainless steel wires with 2 mm exposed at the tips (Cooner Wire, Chatsworth, CA) were placed in the dorsal neck muscles to record electromyogram (EMG). Guide cannulas with stylets (MD-2250; Bioanalytical System) were implanted 2 mm dorsal to the targets in the PH-TMN (A -4.2, L 1.7, H 8.9 mm ventral to dura); PF-LH (A -3.2, L 1.3, H 7.5 mm ventral to dura), and frontal cortex (A 1.2, L 2.5, H 2 mm ventral to dura) for subsequent placement of glutamate sensors (33).

Glutamate sensor data collection. After surgery (1 wk), the rats were habituated to the recording chamber, and sleep-wake states were monitored. A precalibrated glutamate sensor with 1-mm-long active area was inserted through the guide cannula in the PH-TMN, PF-LH, or frontal cortex and fixed firmly to the guide cannula. The sensor was

connected to a four-channel potentiostat (model 3104; Pinnacle Technology) using a flexible cable. The potentiostat was then connected to a personal computer using a USB cable. PAL V1.2.6 software was used (Pinnacle Technology) for acquiring sensor data. Data collection started 2 h after insertion of the glutamate sensor in the brain, at which point a stable baseline was observed. Sleep-wake parameters and glutamate levels were recorded simultaneously (from 11:00 A.M. to 6:00 P.M. during the lights on period) in freely moving rats. Data were collected during spontaneous active waking (AW), quiet wake (QW), NREM sleep, REM sleep, and sleep deprivation. Sleep deprivation studies were performed on the second day. We used only sensor readings taken from the first 2 days after implanting the sensor. We found that, beyond the second day, the sensitivity of the sensor dropped substantially in many cases.

An experiment was conducted to compare glutamate changes recorded using the glutamate sensor with glutamate release using microdialysis-HPLC, across sleep-wake states. In three rats, along with the glutamate sensor cannulas (21-gauge guide, nonsteel), cannulas for microdialysis probes (20-gauge guide, stainless steel) were also implanted in the PH-TMN. The microdialysis guide cannula (blocked with a stylet) was implanted 0.4–0.6 mm lateral (center to center) to the glutamate sensor cannula.

Microdialysis protocol. After 7 days of postoperative recovery, the rats with microdialysis cannulas were habituated to the rodent microdialysis bowl (Bioanalytical Systems, West Lafayette, IN) and to the flexible EEG and EMG recording cables connected to commutators (Plastics One, Roanoke, VA) that were connected to a Grass polygraph. The day before the recording session (16 h before the experiment), the stylets were removed, and a microdialysis probe was placed through the guide cannula. Microdialysis probes (molecular cut-off size of 50 kDa; AI-01 Eicom) with a semipermeable membrane tip length of 1 mm and an outer diameter of 0.22 mm were used. The length of the probe was set so that the glutamate sensor was 0.4–0.6 mm lateral to the semipermeable membrane, and the estimated dialysis field of the probe included the extracellular environment of the glutamate sensor. The microdialysis probe and glutamate sensor were fixed firmly (dental cement) to minimize tissue trauma and to ensure maximum stability of recording. On the day of the experiment, a glutamate sensor was inserted through the guide cannula in the PH-TMN and fixed to the cannula. Next, the adjoining dialysis probe was continuously perfused with artificial cerebrospinal fluid (aCSF; in mM: 145 NaCl, 2.7 KCl, 1.0 $MgCl_2$, 1.2 $CaCl_2$, and 2.0 Na_2HPO_4, pH 7.4) at a flow rate of 2 μl/min by a microinjection pump (Bioanalytical Systems). The time taken for the aCSF solution to travel from the tube to the tip of the microdialysis probe was previously determined.

Microdialysis and glutamate sensor recordings. Data collection started 2 h after insertion of the glutamate sensor in the brain when a stable baseline was observed. Microdialysis samples were collected simultaneously at 5-min intervals (10 μl) using a refrigerated fraction collector (Eicom, Kyoto, Japan). Earlier published studies have reported that 2 h of aCSF perfusion is optimal for achieving a stable measurement of neurotransmitter release (19, 20). The polyethylene collection vials were maintained at 5°C during collection and then stored at −80°C until analyzed. The recovery rate of the microdialysis probes for glutamate was 10–14%. A minimum of three microdialysis samples for each sleep-wake episode were collected.

HPLC assay of glutamate. The concentration of glutamate in the dialysate was detected by HPLC (EP-300; Eicom) with fluorescent detection (excitation/emission = 340/440 nm; Soma S-3350), as described in our prior studies (19, 20, 28). The sample was injected using an autoinjector (ESA 540; ESA, Clemsford, MA). Precolumn derivatization was performed with *o*-phthaldialdehyde/2-mercaptoethanol at 5°C for 3 min. The derivatives were then separated in a liquid chromatography column (MA-5ODS, 2.1 × 150 mm, Eiom) at 30°C with 30% methanol in 0.1 M phosphate buffer (pH 6.0), degassed by an online degasser (DG-100; Eicom). Quantification was achieved with a PowerChrom analysis system (AD Instruments) using external amino acid standards (Sigma). Neurotransmitter concentrations were calculated by comparing the HPLC peak of glutamate in the microdialysis samples with peak areas of known concentrations of glutamate analyzed on the same day. The detection limit for glutamate is 20 fmol.

Recording of sleep-wake stages. Signals for the assessment of different sleep-wake stages (EEG and EMG) were amplified with a Grass model 78E Polygraph (Grass Instruments, Quincy, MA). All recordings were carried out between 11:00 A.M. and 6:00 P.M. during the lights on period. EEG and EMG signals were digitized using a CED 1401 Plus interface and analyzed manually using Spike2 software (Cambridge Electronic Design, Cambridge, UK). Sleep-wake stages were classified based on electrophysiological parameters as previously described (18). In AW, the animal is alert with movements, low-voltage (desynchronized) EEG, increased levels of muscle tone, and frequent eye movements. In QW, the animal shows limited movement and often rests on the ground with low-voltage EEG and low EMG. NREM sleep is characterized by slow wave activity and low EMG (further reduced from QW). REM sleep is characterized by low voltage EEG, muscle atonia, and theta activity.

Glutamate changes with sleep deprivation. Changes in glutamate levels before, during, and after sleep deprivation were recorded by glutamate sensors placed in the PH-TMN, PF-LH, or cortex. EEG and EMG recordings were also performed in this group of animals. Eleven rats (5 for PH-TMN, 3 for PF-LH, and 3 for cortex) were subjected to sleep deprivation starting at 11:00 A.M. for periods ranging from 20 to 120 min. Sleep deprivation was performed by gentle handling, which includes cage tapping and brushing the fur with a cotton tip applicator each time the animal showed signs of sleepiness. Sleep-wake states were monitored by electrophysiological parameters and visual observation.

Histology. Rats were deeply anesthetized with pentobarbital sodium (60 mg/kg), and transcardial perfusion was performed with normal saline followed by 4% buffered paraformaldehyde. After treatment with 30% sucrose in 0.1 M PBS, the brains were cut at 40-μm intervals using a microtome. Cresyl violet staining was done to verify placement of glutamate sensors and dialysis probes.

RESULTS

We used a glutamate sensor (enzyme-based biosensor; Pinnacle Technology) for the measurement of rapid changes in extracellular concentrations of brain glutamate in freely behaving rats. This enzymatic glutamate biosensor [platinum (Pt)-iridium (Ir) electrode] with an integrated Ag/AgCl reference electrode relies on the glutamate oxidase catalyzed conversion of glutamate and O_2 to α-ketoglutaric acid and H_2O_2 (16). The enzymatically produced H_2O_2 is detected by its oxidation with an applied potential of 600 mV at Pt-Ir electrodes. Electroactive interferants present in the brain that are oxidized at the same working potential are eliminated by means of a passive selective membrane composed of nafion and cellulose acetate by coimmobilization of ascorbic acid oxidase. This sensor allows the measurement of physiological extracellular concentrations of glutamate with high sensitivity at low concentrations (μM). This electrode has sensing cavity dimensions of 180-μm diameter and 1.0 mm length, with sensitivity of >3nA/10 μM glutamate. It has a fast response time (1–4 s) allowing the monitoring of the physiological time course of glutamate release.

Before implanting the glutamate sensor, an in vitro precalibration was performed using glutamate and ascorbic acid. Changes in glutamate levels were recorded as changes in electrical current. A linear response to glutamate over the concentration range of 0–50 μM was observed (Fig. 1).
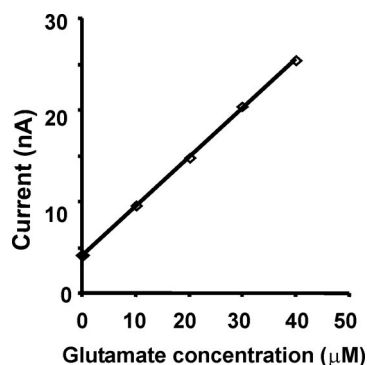
Fig. 1. Calibration of glutamate sensor was performed (in vitro) before in vivo implantation. A linear change in the current was seen with glutamate (10 μM) over the concentration range of 0–50 μM in the representative example presented here. A rapid (1- to 4-s) response in the sensor varying from 3.2 to 5.5 nA/10 μM glutamate was obtained.

Changes in glutamate levels in the regions we studied were well within the detection limit of the glutamate biosensor. We and other investigators, using various techniques, showed that glutamate levels across different brain regions never exceeded 50 μM in rats (2, 15, 19, 28, 40).

Only those sensors that responded by at least 3 nA/10 μM glutamate and did not respond to ascorbic acid (250 μM) were used for in vivo experiments. A rapid (1–4 s) response of the sensors varying from 3.2 to 5.5 nA/10 μM glutamate was obtained. A postexperiment calibration was performed immediately following removal of the sensor, after the in vivo experiments. Four out of five AW and REM sleep states, across all the brain regions studied, showed consistent state-related changes in glutamate release using the glutamate biosensor.

Recordings of sleep-wake stages with Spike 2 software were started simultaneously with PAL software for recording glutamate changes. Based on the calibration of each sensor (Fig. 1), we converted PAL data (pA) to micromolar concentrations of glutamate during the corresponding sleep-wake states. Six rats were used for PH-TMN and three rats each for cortex and PF-LH. The changes in glutamate levels reported are the means of pooled data from all AW, QW, NREM, and REM states for all rats.

After the completion of the experiment, histological examination of the brain sections verified the location of the glutamate sensors and microdialysis probes in the PH-TMN and glutamate sensors in the PF-LH and frontal cortex (Fig. 2).

The time course of glutamate release was determined as the time taken from the "start" to the "peak" glutamate levels (as shown in Fig. 3). The start is defined as the first time point of glutamate increase (>20 pA) from a stable baseline (<10 pA variation over 20 s). The peak is the point of inflection at the beginning of the plateau (>20 pA variation at consecutive data points over 20 s). The time course of glutamate clearance was determined as the time taken from the "drop" to the "postbasal" glutamate levels. The drop is the first time point of glutamate decrease (>20 pA) at the end of the plateau. The postbasal period is the first time point of glutamate return to a stable postbasal reading lasting at least 20 s. The duration of increased glutamate levels was defined as the time taken from the start to the drop in glutamate levels.

Baseline glutamate concentration was taken as the average of the 20 s before the start of each state-dependent glutamate change. This reduces the effect of any circadian influence and any gradual decline in the sensitivity of the sensor. The highest glutamate concentration was determined as the average values from the peak to the drop in glutamate levels. The increase in glutamate concentration was then calculated as the difference between the highest and the baseline readings.

The latency of glutamate changes relative to the onset of each sleep-wake state was calculated as the time difference between the onset of the state and the start of increased glutamate levels. The latency of glutamate changes relative to the offset of each sleep-wake state was calculated as the time difference between the offset of the state and the drop in glutamate levels.

PH-TMN. We observed a marked increase in glutamate levels in the PH-TMN coinciding with the onset of REM sleep compared with NREM sleep (Fig. 3A). The average increase in glutamate concentration in REM sleep was 0.36 ± 0.04 μM above that of the prior NREM sleep period (46 episodes, 6 rats). The start of the increase in glutamate levels was tightly linked (0.6 ± 1.8 s) to the onset of REM episodes (i.e., onset of EEG theta activity and muscle atonia, Figs. 3 and 4). The start of the drop in glutamate levels preceded REM sleep offset by 8.0 ± 3.3 s (Figs. 3 and 4). The magnitude of the increase in glutamate levels was not correlated with the duration of REM sleep. However, there was a high correlation between the duration of increased glutamate levels (from start to drop) and the duration of REM sleep [$r = 0.92$, degrees of freedom (df) 45, $P < 0.0001$; Fig. 3B]. The time taken for glutamate levels to fall from peak to basal values (22.4 ± 4.0 s) with REM sleep
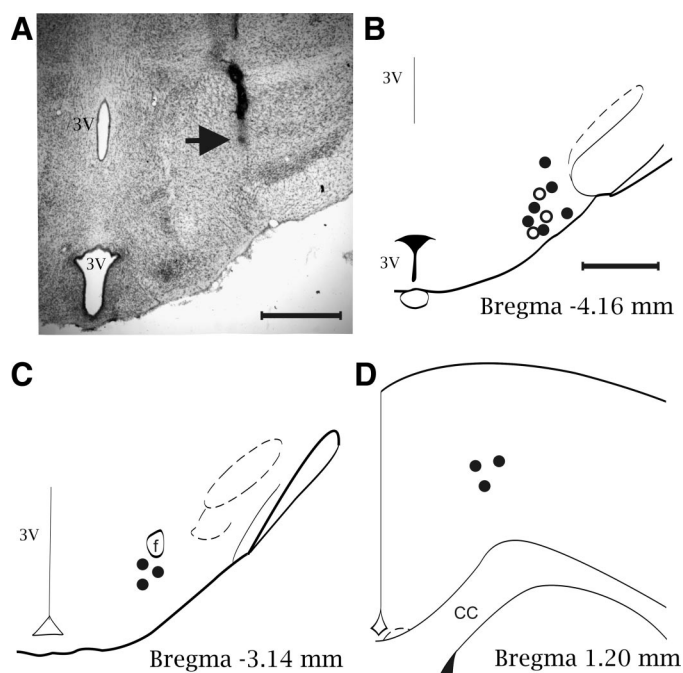

Fig. 2. Location of glutamate sensors. *A*: photomicrograph of the posterior hypothalamic region showing the location of the glutamate sensor. Arrow indicates the location of the tip of the sensor. Location of the glutamate sensors (●) and microdialysis probes (○) in stereotaxic planes of rat brain through the posterior hypothalamus histaminergic tuberomammillary nucleus (PH-TMN; *B*) and glutamate sensors (●) in the perifornical-lateral hypothtlamus (PF-LH; *C*) and the cortex (*D*). Scale bar = 1 mm; scale bar *B* is the same for *C* and *D*. 3V, third ventricle; cc, corpus callosum; f, fornix.
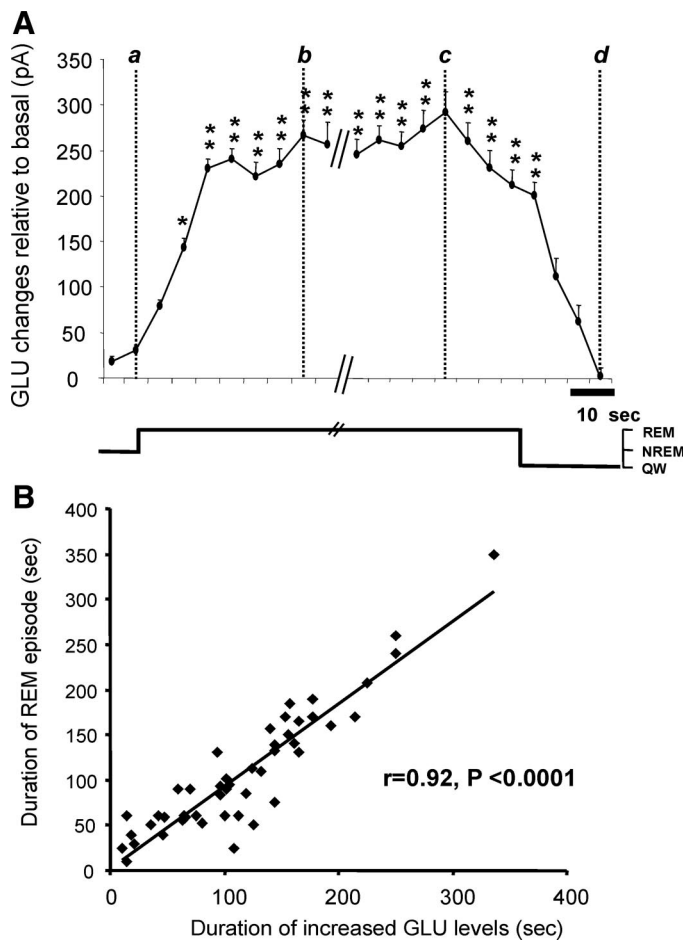
Fig. 3. Changes in glutamate levels in the PH-TMN with the onset and offset of rapid eye movement (REM) sleep. *A*: representative graph showing average glutamate values ± SE of 8 REM sleep episodes (mean duration 120 ± 14.8 s) recorded from one animal. Glutamate levels increased with REM sleep onset and decreased before REM sleep offset [$F = 4.1$, degrees of freedom (df) 7,224, $P < 0.0001$, one-way ANOVA; *$P < 0.05$ and **$P < 0.01$ compared with prior nonrapid eye movement (NREM) sleep levels; Fisher's least-significant difference (LSD)]. *a*, Time point of "start" of glutamate increase; *b*, time point of glutamate "peak"; *c*, time point of glutamate "drop"; *d*, time point of glutamate return to basal levels. *B*: duration of REM sleep and the duration of increased glutamate level significantly correlated.

period (140.3 ± 40.8 s) was nonsignificantly longer than the time taken for glutamate levels to return to basal values in the subsequent state (89.5 ± 15.8 s; Table 1).

Short periods of sleep deprivation by gentle handling (20–120 min) produced gradual increases in glutamate levels in the PH-TMN. Glutamate sensor data showed that glutamate levels peaked 15–20 min after the initiation of sleep deprivation (forced waking). Glutamate levels increased up to 1.51 μM from basal values. Termination of sleep deprivation led to a gradual reduction in glutamate levels. Spontaneous waking increased glutamate levels by 0.32 μM.

Glutamate levels in microdialysis samples collected during REM sleep were higher than those collected during AW and NREM sleep (AW = 2.3 ± 0.12; NREM = 2.4 ± 0.06, REM = 2.5 ± 0.17 pmol/sample). However, these differences were not statistically significant. Microdialysis samples from the PH-TMN also showed a nonsignificant increase in gluta-

offset was similar to the time taken for glutamate levels to increase from start to peak values (27.7 ± 4.2 s) with REM sleep onset (Table 1).

Variation in glutamate levels was calculated relative to AW onset and offset (Fig. 5). We observed that glutamate levels started to increase after the onset of AW (5.4 ± 15.7 s) but started to decrease before the offset of AW (47.2 ± 25.6 s). Glutamate levels increased in AW by 0.32 ± 0.05 μM compared with the preceding state. The magnitude of the relative changes in glutamate levels with AW was similar when AW was preceded by either NREM or QW. We did not observe any changes in glutamate levels linked with muscle tone. There was a high correlation between the duration of AW and the duration of increased glutamate levels ($r = 0.91$, df 16, $P < 0.0001$; Fig. 6*A*). The magnitude of increase in glutamate levels was also significantly correlated with the duration of AW ($r = 0.63$, df 16, $P < 0.01$; Fig. 6*B*). The time taken for glutamate levels to reach peak values after onset of an AW
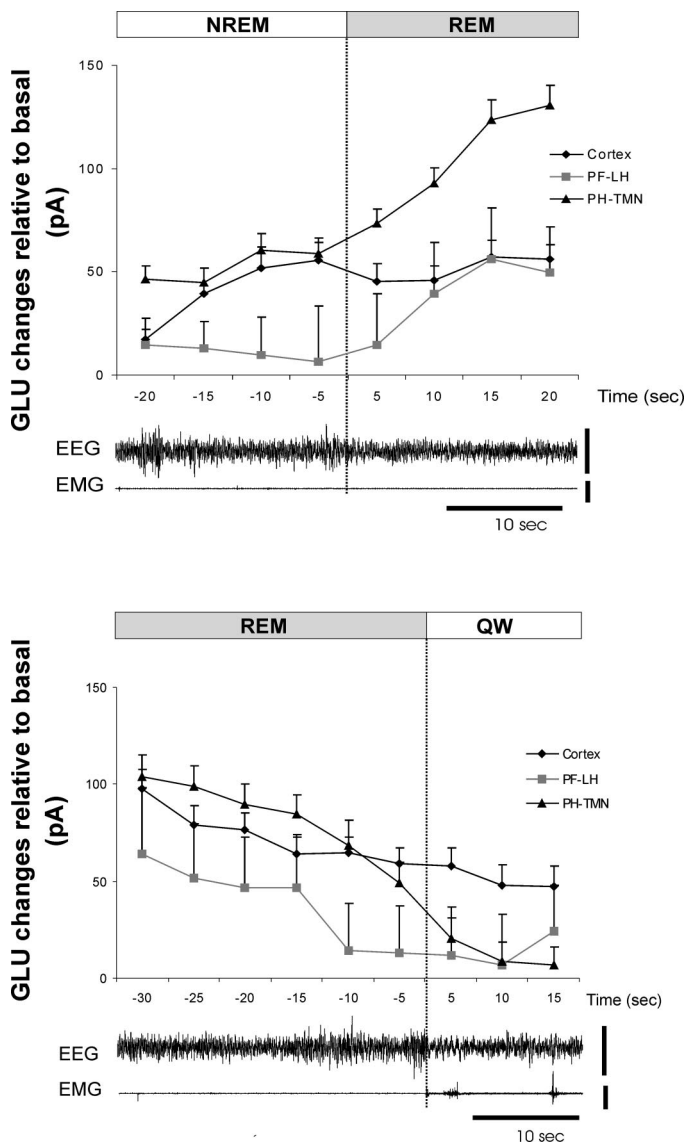

Fig. 4. Changes in glutamate levels are shown at REM sleep onset and offset. Average glutamate levels from different brain regions with REM sleep onset (*top*) and offset (*bottom*). Calibration bars: electroencephalogram (EEG), 50 μV; electromyogram (EMG), 100 μV. QW, quiet waking.

Table 1. *Duration of GLU changes during REM sleep and active waking in different brain regions*

Brain Regions	GLU Start to Peak	GLU Drop to Baseline	Difference, %
REM sleep			
PH-TMN	27.7±4.2	22.4±4.0	−19.1‡
PF-LH	20±6.5	26.7±6.7	33.5§
Cortex	42.4±6.6*	20.3±3.5	−52.1‡
Active waking			
PH-TMN	140.3±40.8	89.5±15.8	−36.2‡
PF-LH	8.6±1.3†	16.7±3.8	94.2§
Cortex	120.6±21.0†	68.1±12.3	−43.5‡

Values(s) are means ± SE. REM, rapid eye movement; PH-TMN, posterior hypothalamus histaminergic tuberomammillary nucleus; PF-LH, perifornical-lateral hypothalamus. Start to peak, duration of glutamate (GLU) increase from start to peak as described in Fig. 3*Ab-a*; drop to baseline, duration of GLU decrease from drop to basal as described in Fig. 3*Ad-c*; difference, GLU drop to baseline/GLU start to peak. †$P < 0.05$ and *$P < 0.01$ compared with drop to base line, *t*-test. ‡Shorter time for glutamate to drop to basal compared with increase (start to peak) from baseline. §Longer time for glutamate to drop to basal compared with increase (start to peak) from baseline.

mate levels with sleep deprivation compared with spontaneous waking (2.8 ± 0.02 vs. 2.5 ± 0.04 pmol/sample). These results are consistent with results obtained with the glutamate biosensor, although they lack its temporal resolution (Fig. 7).

PF-LH. The highest glutamate levels in the PF-LH were observed during AW compared with NREM sleep (27 episodes from 3 rats; Fig. 8*A*), as in the PH-TMN. There was a high correlation between AW duration and the duration of increased glutamate levels ($r = 0.91$, df 26, $P < 0.0001$; Fig. 8*B*). The time taken for glutamate levels to decrease at the offset of AW was significantly longer than the time taken for it to increase at the onset of AW (16.7 ± 3.8 vs. 8.6 ± 1.3 s, $t = 2.0$, df 54, $P < 0.05$; Table 1).

Glutamate levels increased in REM sleep (by 0.42 ± 0.09 μM) compared with the prior NREM sleep periods. This was also observed in the PH-TMN. Sleep deprivation produced a nonsignificant increase in glutamate levels compared with spontaneous AW (0.50 ± 0.08 μM with sleep deprivation vs. 0.52 ± 0.05 μM in AW).

Frontal cortex. Glutamate levels in the frontal cortex increased with AW (16 episodes) and REM sleep (16 episodes) compared with NREM sleep (from 3 rats; Fig. 9*A*). Similar findings were observed in the PH-TMN and PF-LH. There was a significant correlation between AW duration and the duration of increased glutamate levels ($r = 0.67$, df 15, $P < 0.01$; Fig. 9*B*). Sleep deprivation increased glutamate levels significantly more than spontaneous AW [0.72 ± 0.14 μM with sleep deprivation vs. 0.35 ± 0.05 μM in AW; $t = 3.0$, df 21, $P < 0.007$]. REM sleep duration was also significantly correlated with the duration of increased glutamate levels ($r = 0.65$, df 15, $P < 0.01$). The time taken for glutamate levels to increase with AW was significantly longer than the time taken for glutamate levels to decrease to basal levels (120.6 ± 21.0 vs. 68.1 ± 12.3 s; $t = 2.2$, df 30, $P < 0.03$; Table 1). This was also the case in REM sleep (42.4 ± 6.6 vs. 20.3 ± 3.5 s; $t = 3.0$, df 32, $P < 0.005$; Table 1).

The time taken for glutamate levels to increase from "start to peak" and to decrease from "drop to baseline" was faster in the PF-LH compared with both the PH-TMN and the frontal

cortex. Furthermore, glutamate levels increased at a faster rate than it decreased during REM/AW onset and offset in the PF-LH. This is in contrast to the faster decrease in glutamate levels compared with its increase in the PH-TMN and frontal cortex (Table 1).

Analysis of variance of the changes in glutamate levels and of the time course of glutamate variation at REM sleep onset (20 s before and 20 s after REM onset in 5-s periods) showed a significant difference in glutamate levels across the three brain regions [$F(2,92) = 9.2$, $P < 0.0001$, ANOVA]. There was also a significant effect of time course on glutamate levels [$F(7,322)=40.8$, $P < 0.0001$, ANOVA] and the interaction of these two variables [$F(14,644) = 9.6$, $P < 0.0001$, ANOVA]. On the other hand, at REM sleep offset (30 s before and 15 s after the REM offset), glutamate
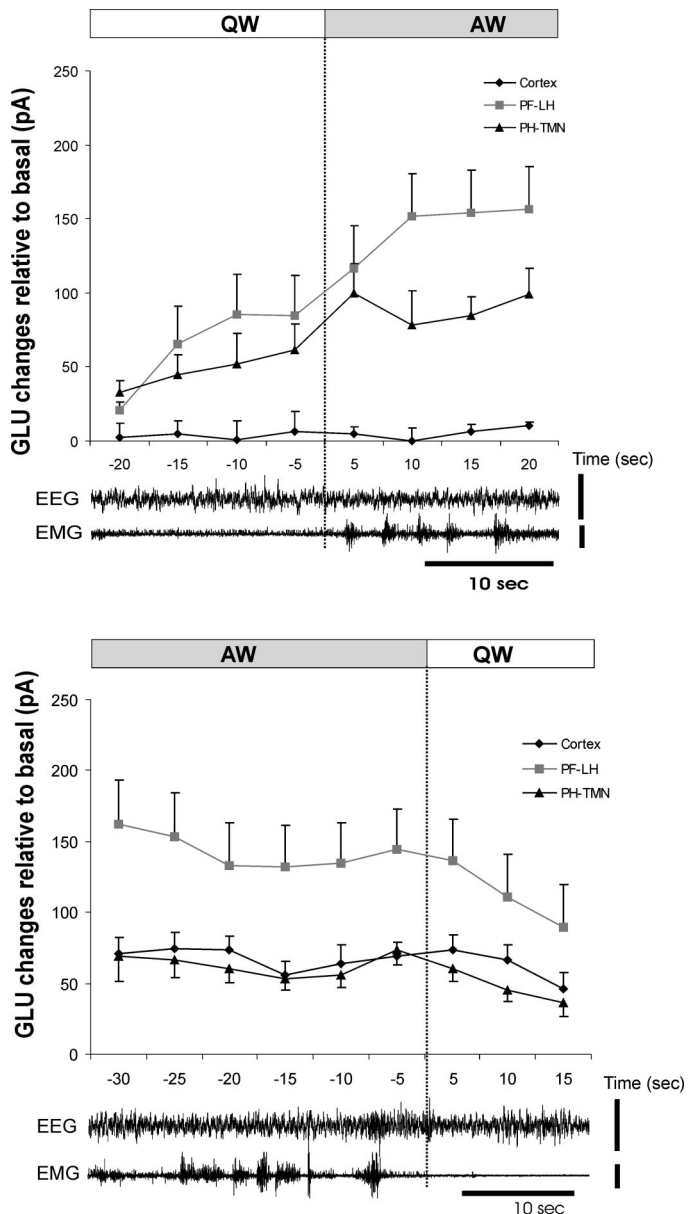

Fig. 5. Changes in glutamate levels are shown with active wake (AW) onset and offset. Average glutamate levels from different brain regions with AW onset (*top*) and offset (*bottom*). Calibration bars: EEG, 50 μV; EMG, 100 μV.
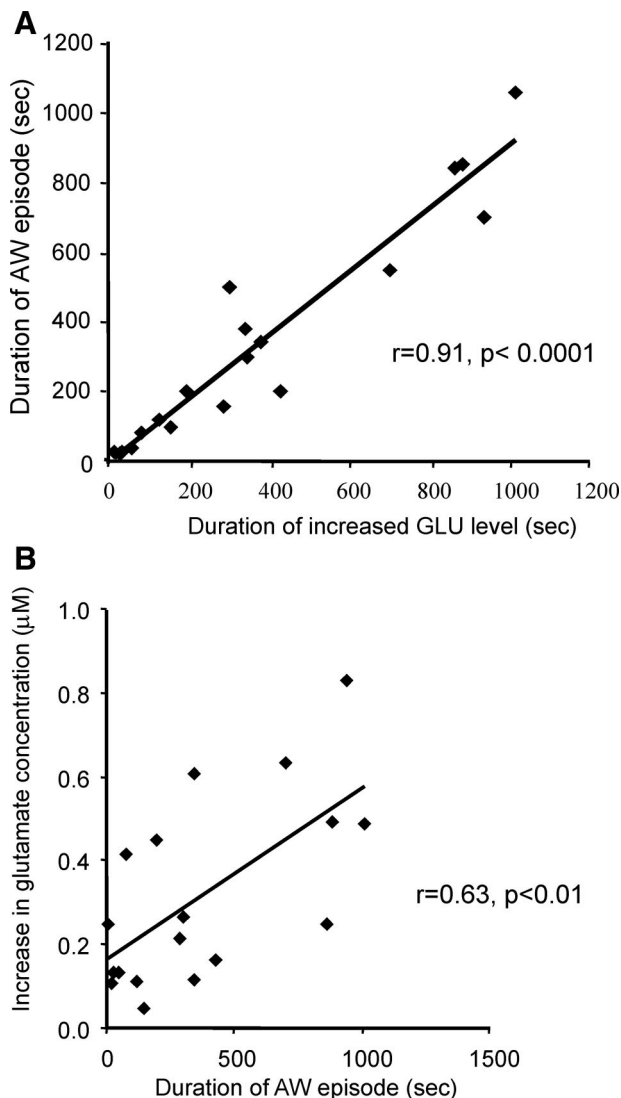
A

B

Fig. 6. Changes in glutamate levels in the PH-TMN during AW. *A*: duration of AW and duration of increased glutamate levels were significantly correlated. *B*: amount of glutamate increase was correlated with the duration of AW.
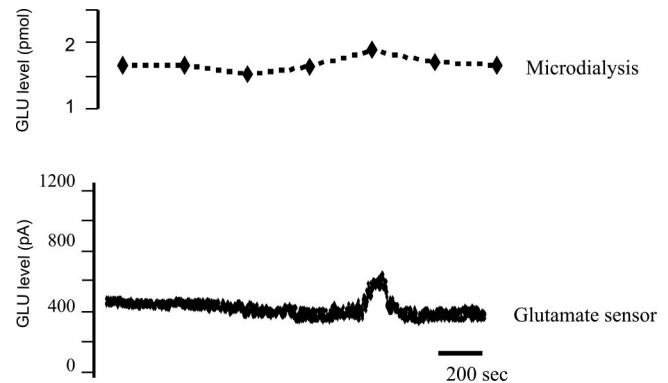

Fig. 7. Microdialysis and glutamate sensor data were collected simultaneously from the PH-TMN. Changes in glutamate levels with microdialysis-HPLC analysis of samples collected every 5 min is given in *top* while time-matched data (collected every s) obtained from the glutamate sensor is on *bottom*. Increased glutamate level measured with the glutamate sensor corresponds to increased glutamate level measured in the microdialysis samples.

DISCUSSION

We observed increased glutamate levels with AW and REM sleep compared with NREM sleep. The increase in glutamate levels strongly coincided with REM sleep onset (0.6 ± 1.8 s) and less strongly with AW onset (5.4 ± 15.7 s) in the PH-TMN. Decreased glutamate levels preceded the offset of AW and REM sleep. These findings suggest that processes linked to reduced glutamate levels may be involved in the termination of AW and REM sleep states.

Glutamate is not enzymatically broken down in the synaptic cleft; however, evidence suggests that most free glutamate is cleared from the cleft very rapidly (10, 47), perhaps within 1

A

B
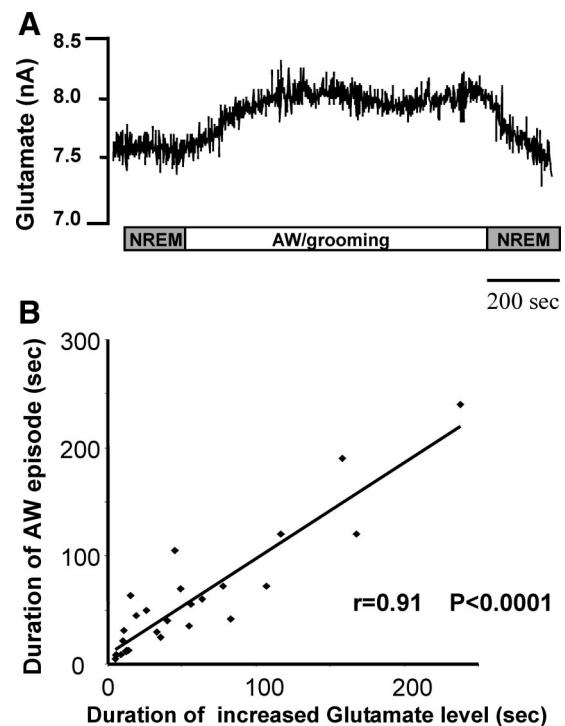
Fig. 8. Changes in glutamate levels in the PF-LH during AW period. *A*: glutamate levels increased with AW and decreased with QW/NREM sleep. *B*: duration of AW and duration of increased glutamate levels were significantly correlated.

levels did not differ significantly across the three brain regions. The effect of time course on glutamate levels [$F_{(8,368)} = 30.3$, $P < 0.0001$, ANOVA] and the interaction of these two variables [$F_{(16,736)} = 7.7$, $P < 0.0001$, ANOVA], however, were significant.

Analysis of variance of the changes in glutamate levels at AW onset showed there was no significant difference in glutamate levels (20 s before and 20 s after the AW onset) across the different brain regions. However, there were significant effects of time on glutamate levels [$F_{(7, 231)} = 7.2$, $P < 0.0001$, ANOVA] and a significant interaction of these two variables [$F_{(14, 462)} = 2.8$, $P < 0.0006$, ANOVA]. In contrast, AW offset (30 s before and 15 s after the AW offset) showed no significant difference in glutamate levels across brain regions. However, there were significant effects of time on glutamate levels [$F_{(8,256)} = 10.2$, $P < 0.0001$, ANOVA] and a signifcant interaction of these two variables [$F_{(16,512)} = 1.6$, $P < 0.05$, ANOVA].
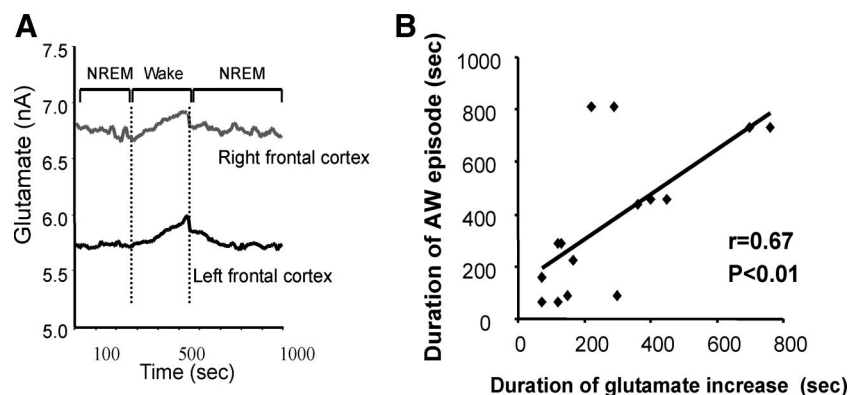
Fig. 9. Changes in glutamate levels in the frontal cortex during AW. *A*: glutamate levels increased in the left and right frontal cortex (recorded simultaneously) with AW and decreased with QW/NREM sleep. *B*: duration of AW and duration of increased glutamate levels were significantly correlated.

ms (6). In theory, such rapid clearance might be accomplished by diffusion alone (49). However, a study by Tong and Jahr (45) suggested that binding to glutamate transporters speeds the clearance of free glutamate. This rapid turnover of glutamate may not be detectable by the standard microdialysis-HPLC techniques, which require much longer duration samples.

Simultaneous glutamate measurements by microdialysis and by the glutamate biosensor were recorded in the PH-TMN. Consistent with the findings of Nitz and Siegel (28), we did not observe any significant variation in glutamate levels across sleep-wake states using the microdialysis technique. This lack of state-related glutamate change could be due to the greater temporal and spatial resolution of the glutamate biosensor compared with the microdialysis technique. This study demonstrates for the first time an increased release of glutamate with REM sleep onset and a decreased release of glutamate before the offset of REM sleep in the PH-TMN. These changes would not have been observable with microdialysis measurement, because the REM duration (1–3 min) in rats is shorter than the normal microdialysis sample collection period (3–5 min).

Hu et al. (16) reported that the glutamate sensor responded to glutamate with a much higher selectivity compared with other interferents, including neurotransmitters [dopamine, norepinephrine, serotonin, γ-aminobutyric acid (GABA)], various metabolites (3,4-dihydrophenyl acetic acid; 4-hydroxy-3-methoxyphenylacetic acid, 3-methoxy-4-hydroxy-phenylglycol, and 5-hydroxyindolacetic acid), and other endogenous electroactive species (L-tyrosine, L-cysteine, L-tryptophan, and L-glutathione). They also showed that there was little or no immediate response when these interferents were added to PBS to mimic in vivo extracellular fluid concentration. Hu et al. (16) went on to show that local microinjections of exogenously applied glutamate in the dentate gyrus of the rat hippocampus, adjacent to the sensor, resulted in an immediate increase in glutamate sensor readings that peaked within seconds of the application. These authors also showed that local application of potassium chloride solution resulted in increased hippocampal glutamate levels as measured by this sensor. Also, electrical stimulation of the perforant (glutamatergic) pathway consistently elicited a peak glutamate sensor reading, whereas a "blank" electrode (identical to the glutamate sensor except without glutamate oxidase) located adjacent to the glutamate electrode showed no change in response to the electrical stimulation of the perforant pathway. These findings demonstrate the selectivity and specificity of the glutamate biosensor in vitro as well as in vivo.

The activity of HA cells of the PH-TMN is highest in waking and lowest in REM sleep (20, 43, 48). We found high glutamate levels in the PH-TMN during both AW and REM sleep compared with NREM sleep. Recent work showed that simultaneous saporin-induced lesions of the HA-, acetylcholine-, and norepinephrine-containing neurons had little effect on the duration of waking (4). The present results suggest that widespread glutamate release may be sufficient to mediate waking, even in the absence of these cell populations. In the intact animal, glutamate release is likely to have a major role in activating these wake-promoting cell groups.

The PH-TMN receives glutamatergic afferent projections from the prefrontal cortex, lateral preoptic area, and lateral hypothalamus (5, 13, 46, 50). Glutamatergic projections may directly activate PH-TMN histaminergic neurons. Hypocretin neurons densely innervate the soma and proximal dendrites of the TMN cells (6). Torrealba et al. (46) showed colocalization of Hcrt and glutamate in axon terminals in the TMN in rats. Most of the Hcrt-immunoreactive terminals in the PH-TMN are glutamatergic and form typical asymmetric, excitatory synapses primarily on the cell bodies and proximal dendrites of PH-TMN neurons (46). The proximity of the glutamatergic vesicles to the synaptic complex suggests that, when these PF-LH neurons fire at low frequency, glutamate neurotransmission should predominate. However, when they fire at higher frequency, the additional release of Hcrt from nonjunctional dense-core vesicles would presumably reinforce the excitation (46). Hcrt exerts a wake-promoting effect through the histaminergic system (17). The effect of Hcrt-1 in waking is linked to glutamate release from the locus coeruleus and the motor nucleus of the trigeminal in rats (23, 34). Hcrt produces a calcium-dependent glutamate release in certain nuclei of the central nervous system (19).

Glutamate may also modulate the activity of HA neurons through its interaction with other wake-related monoaminergic systems. The PH-TMN receives afferent projections from monoaminergic inputs, originating from the adrenergic, noradrenergic, and serotonergic cell groups of various brain regions (12). The PH-TMN neurons also receive an ascending, presumed cholinergic input from the mesopontine tegmentum (13) that is important in brain arousal mechanisms.

Our findings suggest that the changes in HA cell activity during REM sleep are not a consequence of reduced glutamate release. Rather, like the locus coeruleus and the raphe cells,

which are silent in REM sleep, HA cells may be actively inhibited during sleep (14, 28, 29, 30). We hypothesize that glutamate released during REM sleep may activate GABAergic interneurons within target areas as well as GABAergic projection neurons, thus inhibiting HA cells in the PH-TMN. Moreover, PH-TMN neurons receive strong GABAergic inputs from the diagonal band of Broca, lateral hypothalamus, and the preoptic and ventrolateral preoptic regions (36, 37, 41, 51). GABA released from these sites can inhibit TMN neurons by acting on both $GABA_A$ and $GABA_B$ receptors (42, 51). Galanin, which is colocalized with GABA from preoptic projection neurons, may also contribute to the inhibition of HA neurons during REM sleep (37). Increased GABA release in the PH has been reported during REM sleep (28). Nishibori et al. (27) and Oishi et al. (31) reported that GABA agonists decreased the turnover of HA in mouse brain. These findings suggest that increased levels of GABA may override any direct effects of glutamate on HA neurons during REM sleep.

Increased glutamate levels during AW and REM sleep were also seen in the cortex. A recent report using microdialysis also demonstrated an increase in the concentration of glutamate in the rat orbitofrontal cortex during REM sleep (26). We also found increased glutamate levels during AW and REM sleep in the PF-LH. PF-LH Hcrt neurons are involved in the regulation of sleep-wake function (9, 38, 39). Li et al. (25) showed that Hcrt-mediated excitation of local glutamatergic neurons can increase Hcrt neuronal activity, in part by presynaptic facilitation of glutamate release. We found that, in the PF-LH, glutamate levels took a longer time to return to basal values compared with the time it took for glutamate levels to increase to peak values during AW. This is in contrast to the other regions we studied (PH-TMN and frontal cortex) in which the return to basal values at AW offset was quicker than their rise with AW onset. This suggests the possibility of a less robust glutamate clearance mechanism in the PF-LH compared with the PH-TMN and the cortex.

Perspectives and Significance

This study provides evidence of rapid increases in glutamate levels with REM sleep and AW in the PH-TMN, PF-LH, and frontal cortex. The glutamate biosensor is superior to the standard microdialysis-HPLC technique in providing the temporal resolution required for detection and description of sleep-wake-related changes in glutamate concentrations.

REFERENCES

1. **Abrahamson EE, Leak RK, Moore RY.** The suprachiasmatic nucleus projects to posterior hypothalamic arousal systems. *NeuroReport* 12: 435–440, 2001.
2. **Albrecht J, Hilgier W, Zielinska M, Januszewski S, Hesselink M, Quack G.** Extracellular concentrations of taurine, glutamate, and aspartate in the cerebral cortex of rats at the asymptomatic stage of thioacetamide-induced hepatic failure: modulation by ketamine anesthesia. *Neurochem Res* 25: 1497–1502, 2000.
3. **Bettendorff L, Sallanon-Moulin M, Touret M, Wins P, Margineanu I, Schoffeniels E.** Paradoxical sleep deprivation increases the content of glutamate and glutamine in rat cerebral cortex. *Sleep* 19: 65–71, 1996.
4. **Blanco-Centurion C, Gerashchenko D, Shiromani PJ.** Effects of saporin-induced lesions of three arousal populations on daily levels of sleep and wake. *J Neurosc* 27: 14041–8, 2007.
5. **Brown RE, Stevens DR, Haas HL.** The physiology of brain histamine. *Prog Neurobiol* 63: 637–72, 2001.
6. **Chemelli RM, Willie JT, Sinton CM, Elmquist JK, Scammell T, Lee C, Richardson JA, Williams SC, Xiong Y, Kisanuki Y, Fitch TE, Nakazato M, Hammer RE, Saper CB, Yanagisawa M.** Narcolepsy in orexin knockout mice: molecular genetics of sleep regulation. *Cell* 98: 437–451, 1999.
7. **Chu M, Huang ZL, Qu WM, Eguchi N, Yao MH, Urade Y.** Extracellular histamine level in the frontal cortex is positively correlated with the amount of wakefulness in rats. *Neurosci Res* 49: 417–420, 2004.
8. **Clements JD, Lester RA, Tong G, Jahr CE, Westbrook GL.** The time course of glutamate in the synaptic cleft. *Science* 258: 1498–1501, 1992.
9. **de Lecea L, Sutcliffe JG.** The hypocretins and sleep. *Febs J* 272: 5675–5688, 2005.
10. **Diamond JS, Jahr CE.** Transporters buffer synaptically released glutamate on a submillisecond time scale. *J Neurosci* 17: 4672–4687, 1997.
11. **Disbrow JK, Ruth JA.** Differential glutamate release in brain regions of long sleep and short sleep mice. *Alcohol* 1: 201–203, 1984.
12. **Ericson H, Blomqvist A, Kohler C.** Brainstem afferents to the tuberomammillary nucleus in the rat brain with special reference to monoaminergic innervation. *J Comp Neurol* 281: 169–192, 1989.
13. **Ericson H, Blomqvist A, Kohler C.** Origin of neuronal inputs to the region of the tuberomammillary nucleus of the rat brain. *J Comp Neurol* 311: 45–64, 1991.
14. **Gervasoni D, Peyron C, Rampon C, Barbagli B, Chouvet G, Urbain N, Fort P, Luppi PH.** Role and origin of the GABAergic innervation of dorsal raphe serotonergic neurons. *J Neurosci* 20: 4217–4225, 2000.
15. **Guyot LL, Diaz FG, O'Regan MH, McLeod S, Park H, Phillis JW.** Real-time measurement of glutamate release from the ischemic penumbra of the rat cerebral cortex using a focal middle cerebral artery occlusion model. *Neurosci Lett* 299: 37–40, 2001.
16. **Hu Y, Mitchell KM, Albahadily FN, Michaelis EK, Wilson GS.** Direct measurement of glutamate release in the brain using a dual enzyme-based electrochemical sensor. *Brain Res* 659: 117–125, 1994.
17. **Huang ZL, Qu WM, Li WD, Mochizuki T, Eguchi N, Watanabe T, Urade Y, Hayaishi O.** Arousal effect of orexin A depends on activation of the histaminergic system. *Proc Natl Acad Sci USA* 98: 9965–9970, 2001.
18. **John J, Kumar VM.** Effect of NMDA lesion of the medial preoptic neurons on sleep and other functions. *Sleep* 21: 587–598, 1998.
19. **John J, Wu MF, Kodama T, Siegel JM.** Intravenously administered hypocretin-1 alters brain amino acid release: an in vivo microdialysis study in rats. *J Physiol* 548: 557–562, 2003.
20. **John J, Wu MF, Boehmer LN, Siegel JM.** Cataplexy-active neurons in the hypothalamus: implications for the role of histamine in sleep and waking behavior. *Neuron* 42: 619–634, 2004.
21. **John J, Ramanathan L, Siegel JM.** *Rapid Variations in Glutamate Levels Across Sleep-wake States.* Atlanta, GA: Soc Neurosci., Program No 14.4, 2006.
22. **Kodama T, Honda Y.** Acetylcholine and glutamate release during sleep-wakefulness in the pedunculopontine tegmental nucleus and norepinephrine changes regulated by nitric oxide. *Psychiatry Clin Neurosci* 53: 109–111, 1999.
23. **Kodama T, Kimura M.** Arousal effects of orexin-A correlate with GLU release from the locus coeruleus in rats. *Peptides* 23: 1673–1681, 2002.
24. **Kodama T, Lai YY, Siegel JM.** Enhanced glutamate release during REM sleep in the rostromedial medulla as measured by in vivo microdialysis. *Brain Res* 780: 178–181, 1998.
25. **Li Y, Gao XB, Sakurai T, van den Pol AN.** Hypocretin/orexin excites hypocretin neurons via a local glutamate neuron-A potential mechanism for orchestrating the hypothalamic arousal system. *Neuron* 36: 1169–1181, 2002.
26. **Lopez-Rodriguez F, Medina-Ceja L, Wilson CL, Jhung D, Morales-Villagran A.** Changes in extracellular glutamate levels in rat orbitofrontal cortex during sleep and wakefulness. *Arch Med Res* 38: 52–55, 2007.
27. **Nishibori M, Oishi R, Itoh Y, Saeki K.** Effects of GABA-mimetic drugs on turnover of histamine in the mouse brain. *Jpn J Pharmacol* 41: 403–408, 1986.
28. **Nitz D, Siegel JM.** GABA release in posterior hypothalamus across sleep-wake cycle. *Am J Physiol Regul Integr Comp Physiol* 271: R1707–R1712, 1996.
29. **Nitz D, Siegel JM.** GABA release in the locus coeruleus as a function of sleep/wake state. *Neuroscience* 78: 795–801, 1997.

30. **Nitz D, Siegel JM.** GABA release in the dorsal raphe nucleus: role in the control of REM sleep. *Am J Physiol Regul Integr Comp Physiol* 273: R451–R455, 1997.

31. **Oishi R, Nishibori M, Itoh Y, Saeki K.** Diazepam-induced decrease in histamine turnover in mouse brain. *Eur J Pharmacol* 124: 337–342, 1986.

32. **Okakura K, Yamatodani A, Mochizuki T, Horii A, Wada H.** Glutamatergic regulation of histamine release from rat hypothalamus. *Eur J Pharmacol* 213: 189–192, 1992.

33. **Paxinos G, Watson C.** *The Rat Brain in Stereotaxic Coordinates.* San Diego, CA: Academic, 1997.

34. **Peever JH, Lai YY, Siegel JM.** Excitatory effects of hypocretin-1 (orexin-A) in the trigeminal motor nucleus are reversed by NMDA antagonism. *J Neurophysiol* 89: 2591–2600, 2003.

35. **Peyron C, Faraco J, Rogers W, Ripley B, Overeem S, Charnay Y, Nevsimalova S, Aldrich M, Reynolds D, Albin R, Li R, Hungs M, Pedrazzoli M, Padigaru M, Kucherlapati M, Fan J, Maki R, Lammers GJ, Bouras C, Kucherlapati R, Nishino S, Mignot E.** A mutation in a case of early onset narcolepsy and a generalized absence of hypocretin peptides in human narcoleptic brains. *Nat Med* 6: 991–997, 2000.

36. **Salin-Pascual R, Gerashchenko D, Greco M, Blanco-Centurion C, Shiromani PJ.** Hypothalamic regulation of sleep. *Neuropsychopharmacology* 25: S21–S27, 2001.

37. **Sherin JE, Elmquist JK, Torrealba F, Saper CB.** Innervation of histaminergic tuberomammillary neurons by GABAergic and galaninergic neurons in the ventrolateral preoptic nucleus of the rat. *J Neurosci* 18: 4705–4721, 1998.

38. **Siegel JM.** Narcolepsy: a key role for hypocretins (orexins). *Cell* 98: 409–412, 1999.

39. **Siegel JM.** Hypocretin (orexin): role in normal behavior and neuropathology. *Annu Rev Psychol* 55: 125–148, 2004.

40. **Silva E, Hernandez L, Quinonez B, Gonzalez LE, Colasante C.** Selective amino acids changes in the medial and lateral preoptic area in the formalin test in rats. *Neurosci* 124: 395–404, 2004.

41. **Steininger TL, Gong H, McGinty D, Szymusiak R.** Subregional organization of preoptic area/anterior hypothalamic projections to arousal-related monoaminergic cell groups. *J Comp Neurol* 429: 638–653, 2001.

42. **Stevens DR, Kuramasu A, Haas HL.** GABAB-receptor mediated control of GABAergic inhibition in rat histaminergic neurons in vitro. *Eur J Neurosci* 11: 1148–1154, 1999.

43. **Takahashi K, Lin JS, Sakai K.** Neuronal activity of histaminergic tuberomammillary neurons during wake-sleep states in the mouse. *J Neurosci* 26: 10292–10298, 2006.

44. **Thannickal TC, Moore RY, Nienhuis R, Ramanathan L, Gulyani S, Aldrich M, Cornford M, Siegel JM.** Reduced number of hypocretin neurons in human narcolepsy. *Neuron* 27: 469–474, 2000.

45. **Tong G, Jahr CE.** Block of glutamate transporters potentiates postsynaptic excitation. *Neuron* 13: 1195–1203, 1994.

46. **Torrealba F, Yanagisawa M, Saper CB.** Colocalization of orexin and glutamate immunoreactivity in axon terminals in the tuberomammillary nucleus in rats. *Neuroscience* 119: 1033–1044, 2003.

47. **Trussell LO, Zhang S, Raman IM.** Desensitization of AMPA receptors upon multiquantal neurotransmitter release. *Neuron* 10: 85–1196, 1993.

48. **Vanni-Mercier G, Gigout S, Debilly G, Lin JS.** Waking selective neurons in the posterior hypothalamus and their response to histamine H3-receptor ligands: an electrophysiological study in freely moving cats. *Behav Brain Res* 144: 227–241, 2003.

49. **Wahl LM, Pouzat C, Stratford KJ.** Monte Carlo simulation of fast excitatory synaptic transmission at a hippocampal synapse. *J Neurophysiol* 75: 597–608, 1996.

50. **Wouterlood FG, Steinbusch HW, Luiten PG, Bol JG.** Projection from the prefrontal cortex to histaminergic cell groups in the posterior hypothalamic region of the rat. Anterograde tracing with Phaseolus vulgaris leucoagglutinin combined with immunocytochemistry of histidine decarboxylase. *Brain Res* 406: 330–336, 1987.

51. **Yang QZ, Hatton GI.** Electrophysiology of excitatory and inhibitory afferents to rat histaminergic tuberomammillary nucleus neurons from hypothalamic and forebrain sites. *Brain Res* 773: 162–172, 1997.